Applied Adhesion Science

RESEARCH Open Access

Adhesively bonded joints of jute, glass and hybrid jute/glass fibre-reinforced polymer composites for automotive industry

H. F. M. de Queiroz, M. D. Banea* and D. K. K. Cavalcanti

*Correspondence:
mdbanea@gmail.com
Federal Center
of Technological Education
of Rio de Janeiro (CEFET/RJ),
Rio de Janeiro, Brazil

Abstract

Natural fibre-reinforced composites have attracted a great deal of attention by the automotive industry mainly due to their sustainable characteristics and low cost. The use of sustainable composites is expected to continuously increase in this area as the cost and weight of vehicles could be partially reduced by replacing glass fibre composites and aluminium with natural fibre composites. Adhesive bonding is the preferred joining method for composites and is increasingly used in the automotive industry. However, the literature on natural fibre reinforced polymer composite adhesive joints is scarce and needs further investigation. The main objective of this study was to investigate experimentally adhesively bonded joints made of natural, synthetic and interlaminar hybrid fibre-reinforced polymer composites. The effect of the number of the interlaminar synthetic layers required in order to match the bonded joint efficiency of a fully synthetic GFRP bonded joint was studied. It was found that the failure load of the hybrid jute/glass adherend joints increased by increasing the number of external synthetic layers (i.e. the failure load of hybrid 3-layer joint increased by 28.6% compared to hybrid 2-layer joint) and reached the pure synthetic adherends joints efficiency due to the optimum compromise between the adherend material property (i.e. stiffness and strength) and a diminished bondline peel stress state.

Keywords: Natural fibres, Synthetic fibres, Hybrid composites, Jute fibre, Glass fibre, Adhesively bonded joints, Automotive industry

Introduction

Adhesively bonded joints have shown to be viable substitutes to classical mechanical joints in various industries (i.e. automotive, aeronautical, marine, sports, among others) [1–4]. Bonded joints present many inherent advantages compared to their classical counterparts (i.e. more uniformly distributed stresses, design flexibility, reduced weight, lower cost, fatigue resistance, damage tolerance, good surface finish, strength to weight ratio, etc.). Fibre reinforced composites (FRC) are increasingly been used in bonded structures in order to reduce structural weight and cost by replacing metal adherends [5, 6], with the focus on glass (GFRP) and carbon fibre (CFRP) reinforced composites. However, natural fibre reinforced composites (NFRC), have been continuously explored as an alternative to synthetic FRCs in many applications, due to their positive characteristics

such as low weight, cost and environmental impact. For instance, NFRCs are nowadays used in non-structural car body parts, such as: door panels, package trays, hat racks, instrument panels, internal engine covers, sun visors, boot liners, oil air filters and even progressing to more structurally demanding parts such as seat backs and exterior underfloor panelling [7]. However, they present some disadvantages (i.e. variable fibre quality and humidity absorption due to a more hydrophilic fibre nature, leading to low fibre/matrix interfacial strength) [8–10]. One of the methods used in the literature to surpass these shortcomings is the hybridization technique, which consists of the application of two or more reinforcement materials in a single matrix [11–13]. Natural reinforcements are beneficial due to the aforementioned eco-friendliness, lower weight and cost, while synthetic reinforcements such as glass, have higher strength, lower water absorption and increased fibre/matrix interfacial strength [14]. For example, the use of jute fibres is related to the attractive strength and toughness properties of this material (between 1/8 and 1/4 of E-glass fibres [15]) and its wide use in several industries. Jute presents higher stiffness than other common natural fibres such as sisal [16]. However, the density of jute is nearly half that of glass fibres (i.e. 1.3 compared to approx. 2.5), which makes it a viable replacement, allowing to match the stiffness of glass fibre components at a smaller weight. On the other hand, the stiffness of jute fibres is nearly 80% that of glass fibres [17] and cost (the cost per weight of jute may achieve 1/9 that of glass fibres). Several studies for the mechanical, thermal and impact characterization of jute fibres and their composites are available in the literature [11–13, 18].

The behaviour of adhesively bonded joints with NFRCs was investigated by several researchers [19–27]. Gonzalez-Murillo and Ansell [21] studied the effect of joint geometry on the strength of natural fiber composite joints using three different geometry types: single lap shear joints (SLJs), co-cured joints termed intermingled fibre joins (IFJs) and laminated fibre joints (LFJs) of henequen and sisal fibre composite. They found that the IFJs and LFJs presented higher lap shear strengths than the single lap shear joints. De Queiroz et al. [20] has shown that intralaminar synthetic hybridization of jute and sisal composites via glass fibre has a significant effect on both adherend material properties and bonded joint strength. Melese et al. [22] investigated the effect of joint configuration and hybridization in pure jute, sisal and jute/sisal hybrid joints using single lap joint, double strap butt joint and scarf-45° joint. The highest joint strength reported was for the hybrid composite joints, while the most efficient joint configuration was found to be the double strap butt joint. Mittal et al. [23] studied the behaviour of jute-based composites while varying the overlap length and curing temperature in single and double lap joints. Delamination was found to be the dominant failure mode. Yoon et al. [26] investigated the effect of bamboo fibre layer positioning on the performance of bonded joints and found that the fibre positioning had a significant effect in stress concentration of the adhesive joint. Ferreira et al. [27] studied the influence of stacking sequence and natural fiber content of s hybrid composite in the fatigue strength of bonded joints and found that the fatigue strength of hybrid stacked joints was lower than the single fiber composite joints due to lower adhesion between hemp and adhesive layer.

The main objective of this study was to investigate experimentally single-lap adhesively bonded joints made of natural, synthetic and interlaminar hybrid fibre-reinforced polymer composites. The effect of the number of the interlaminar synthetic layers required

Table 1 Tensile data of the adhesive and resin used [28–30]

Polymer	Tensile strength (MPa)	Young's modulus (GPa)	Tensile strain (%)
Betamate™2096	34.27 ± 1.52	1.60 ± 0.10	8.04 ± 0.39
HEX 135 SLOW	60.92 ± 1.42	3.25 ± 0.008	3.20 ± 0.20

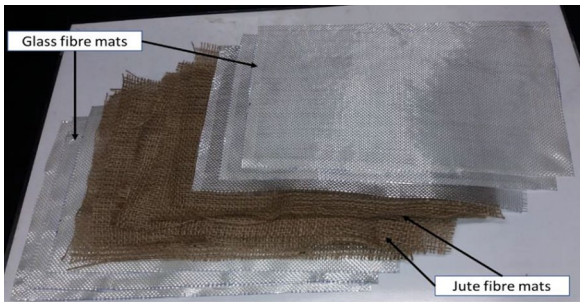

Fig. 1 Natural and synthetic fabrics used and stacking sequence for the fabrication of the hybrid composite adherends 3-layer glass fibre hybrid composite case ($G_3J_5G_3$)

in order to match the bonded joint efficiency of a fully synthetic GFRP bonded joint was studied. SLJs bonded with a modern tough structural adhesive used in the automotive industry were tested.

Materials and methods

Materials

Bidirectional jute and glass plain woven fabrics were used as reinforcements. Jute fabrics (T10, 248 g/m^2) were supplied by Sisalsul (São Paulo, Brazil) while the glass ones (RE200, 200 g/m^2) were supplied by Barracuda Advanced Composites (Rio de Janeiro, Brazil). A two-component epoxy resin, HEX 135 SLOW, supplied by Barracuda Advanced Composites (Rio de Janeiro, Brazil) was used to fabricate the composites.

A structural, two-component epoxy adhesive, Betamate™2096, supplied by Dow (São Paulo, Brazil) was used in the fabrication of the SLJs. The tensile data for the adhesive and resin used are summarized on Table 1.

Composite specimen fabrication

Composite plates (pure synthetic, pure natural and hybrid) were fabricated using the hand lay-up technique followed by hot press compression moulding via a steel mould and a heated plate hydraulic press, Solab SL-20 (São Paulo, Brazil). The curing time was of 8 h at 70 °C as per manufacturer guidelines. Once cured, the adherends were cut from the composite plates (25 × 107.5 mm).

The hybrid composites were fabricated in such a way to have a stacking sequence that had a natural fibre core consisting of 5 layers of jute and an envelope of symmetrical glass fabric layers on either side. The number of glass layers varied on either side from 2 to 3 layers. The fibre weight percentage was kept at around 30% and the resin + hardener (100:33) at 70% of the final composite weight. Figure 1 shows the layer sequence of the

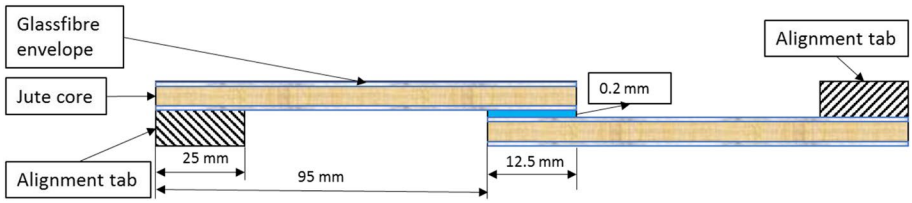

Fig. 2 Joint specimen geometry

natural and synthetic fabrics used for the fabrication of the hybrid composite adherends 3-layer glass fibre hybrid composite case ($G_3J_5G_3$).

The composite materials used as adherends received specific nomenclature as a function of synthetic layer number and stacking sequence (the subscript represents the number of layers):

- GFRP—Glass fibre reinforced composite;
- $G_2J_5G_2$—2-layer glass fibre hybrid composite;
- $G_3J_5G_3$—3-layer glass fibre hybrid composite;
- JFRP—Jute fibre reinforced composite.

The materials used as adherends were characterised by tensile tests using a universal Instron®5966 testing machine (Norwood, Massachusetts, USA). A 10 kN load cell and a crosshead speed of 1 mm/min was used. Tensile stress–strain curves of all composite materials used as adherends were recorded and the calculated tensile data (the tensile strength, Young`s modulus and strain) are summarised in Table 2.

Specimen fabrication

The geometry of the joint specimen can be seen in Fig. 2. A mould with steel spacers was used to maintain the correct alignment of the adherends and avoid spew fillets [31]. The spacers also ensured the adhesive layer thickness of 0.2 mm and the overlap length of 12.5 mm. Alignment tabs were glued to the edges of the SLJs to align the specimen during the traction tests.

The surface of the composite substrates was manually abraded using a 100-grit sandpaper in crisscrossing 45° angles in order to increase the mechanical interlocking of the adhesive/adherend interface as well as to remove impurities and traces of releasing agents [32]. The area to be bonded was then cleaned with 99% acetone in order to avoid adhesive failures due to chemical impurities [1]. The joints were cured via a hydraulic press (model SL-12/20, Solab) for 2 h at 60 °C, as per manufacturer guidelines.

Test methods

All specimens were tested in traction via a universal testing machine INSTRON®5966 at a crosshead speed of 1 mm/min (see Fig. 3). At least four specimens were tested for each case at room temperature. Load–displacement curves were recorded during the test.

Table 2 Tensile data of the composites used as adherends

Adherend material	Tensile strength (MPa)	Young's modulus (GPa)	Tensile strain (%)
GFRP	197.85 ± 19.54	20.16 ± 4.86	2.00
$G_3J_5G_3$	136.30 ± 7.50	10.22 ± 0.24	1.45
$G_2J_5G_2$	100.64 ± 2.39	7.48 ± 0.99	1.24
JFRP	80.02 ± 10.70	7.86 ± 0.74	0.92

After the tests, the failure modes of bonded joints were visually analysed and categorized in accordance to the ASTM 5573 [33].

Results and discussion

Joint failure modes

The failure modes of composite bonded joint may occur either in the adherend (i.e. fibre tear, light fibre tear, thin layer cohesive failure and stock break failure), in the adherend/adhesive interface (adhesive failure) or within the adhesive layer (cohesive failure). Light fibre tear (LFT) and thin layer cohesive failures (TLC) are defined as close to the interface cohesive failures. LFT is defined as the presence of a thick adhesive layer on one side and no adhesive on the other with some surface resin and few fibres removed from the interface. On the other hand, TLC is defined as a thick layer of adhesive on one side and a very thin adhesive layer on the other. Fibre tear failure is also called delamination and is defined as a more severe and widespread fibre removal and bundle failures.

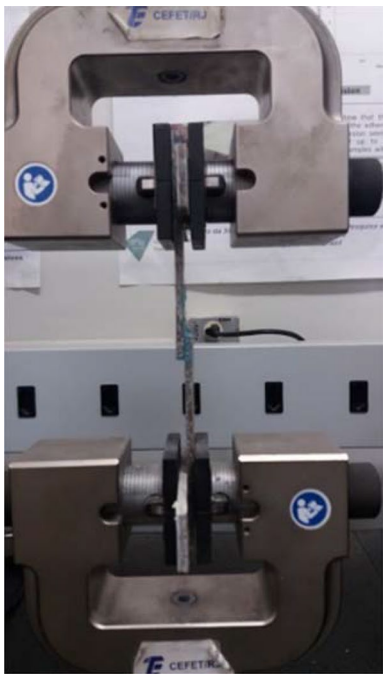

Fig. 3 Tensile test set-up

It is also common the observation of mixed modes, where any of the failure modes may occur alongside one another.

Figure 4 presents representative failure modes for all joints studied. From Fig. 4a, it can be seen that the failure mode of $G_2J_5G_2$ SLJs presented a mix of LFT, TLC and fibre tear (delamination). For the $G_3J_5G_3$ SLJs (see Fig. 4b), it can be seen that the majority of the failure surface was dominated by cohesive failure, mixed with TLC. Figure 4c depicts the failure mode of the GFRP SLJs, where widespread LFT can be seen. Finally, from Fig. 4d, e, the stock break failure of the JFRP SLJs group can be observed. The significant difference, in terms of failure mode, of GFRP and JFRP SLJs, is due to the fact that the jute fibre and its composite is more brittle. This, in turn means that the JFRP is less capable of rotating its edge to account for the increasing peel stress cause by the eccentricity of the load in an SLJ traction test.

For further clarification on the failure mode of the joints, an electronic microscope was used to determine more precisely the failure modes and the transition zones. From Fig. 5, it is possible to see the LFT failure mode that is characteristic of a GFRP bonded joint. Patches of adhesive with some surface fibre removal as well as the removal of surface resin is apparent. The underlying bidirectional glass fabric however is not visible, indicating that this failure occurs very close to the interface. The crack path represents two LFT fronts from each overlap edge that meet in the middle with an extremely

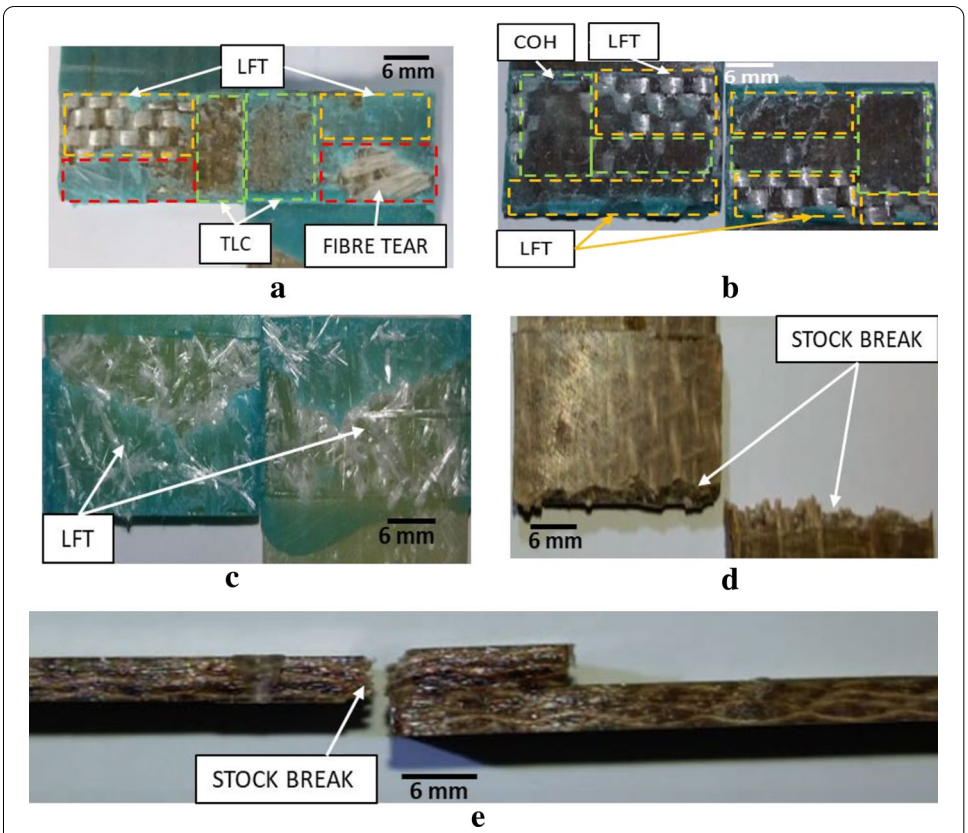

Fig. 4 Representative adhesive joint failure surfaces: **a** $G_2J_5G_2$; **b** $G_3J_5G_3$; **c** GFRP, **d** JFRP (top view) and **e** JFRP (side view)

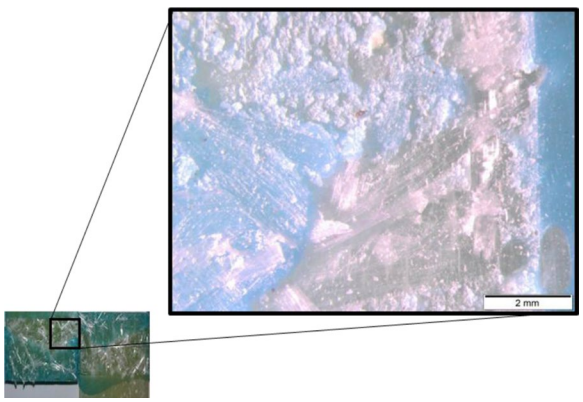

Fig. 5 Microscope image of representative failure mode of GFRP SLJs

narrow transition zone. This failure mode is consistent with what has been previously noted in the literature [34, 35]. Figure 6 presents a detailed view of the hybrid 2-layer bonded joint failure surface. It can be observed from Fig. 6a that the top right zone of the hybrid 2-layer failure surface, roughly 25% of the area, was dominated by a generalized LFT mode. This is due to the clear removal of the surface resin of the other adherend, with the delamination of a few individual fibres. It can also be seen the faint warp/weft directions of the bidirectional mat. From Fig. 6b, one can observe the zone below that of the previously discussed zone. This zone is dominated by a generalized delamination (fibre tear) failure. Fibres of both the first and second layers were delaminated, indicating a significant peel stress state.

Finally, from Fig. 6c, it can be seen that the left half of the failure surface presented a mixed TLC/LFT failure mode. This is due to the lighter adhesive dusting and visible matrix underneath as well as pulled surface resin with the warp and weft direction from the opposite adherend. It is noteworthy that a narrow transition zone is evident between the zones discussed in Fig. 6a and c. In other words, the entire failure surface was close to the adhesive/adherend interface, which means that the crack propagated almost entirely in the multi-material interphase, rather than cohesive within the adhesive, which is a lower energy path. In comparison to the GFRP SLJs failure mode, a faint but apparent warp/weft pattern is visible, indicating that the crack path occurred closer to the adherend.

Figure 7 presents magnification details of the hybrid 3-layer bonded joint failure surface. It can be seen that a stable cohesive crack propagation occurred (see Fig. 7a). This is also a ductile behaviour as depicted by the wavy progression instead of a smooth surface. Figure 7b presents a more LFT oriented (mixed) cohesive failure mode, due to a lower adhesive density on the surface and visible pulled resin and few delaminated surface fibres. Figure 7c presents the most severe form of TLC/LFT mixed mode observed in the case, defined by a more significant surface fibre bundle resin removal and fibre delamination. This is due to higher peel stresses close to the overlap edge. In general, the main difference in failure mode as a function of number of synthetic layers was due to failures closer to the interface and pockets of generalized delamination in the hybrid 2-layer case.

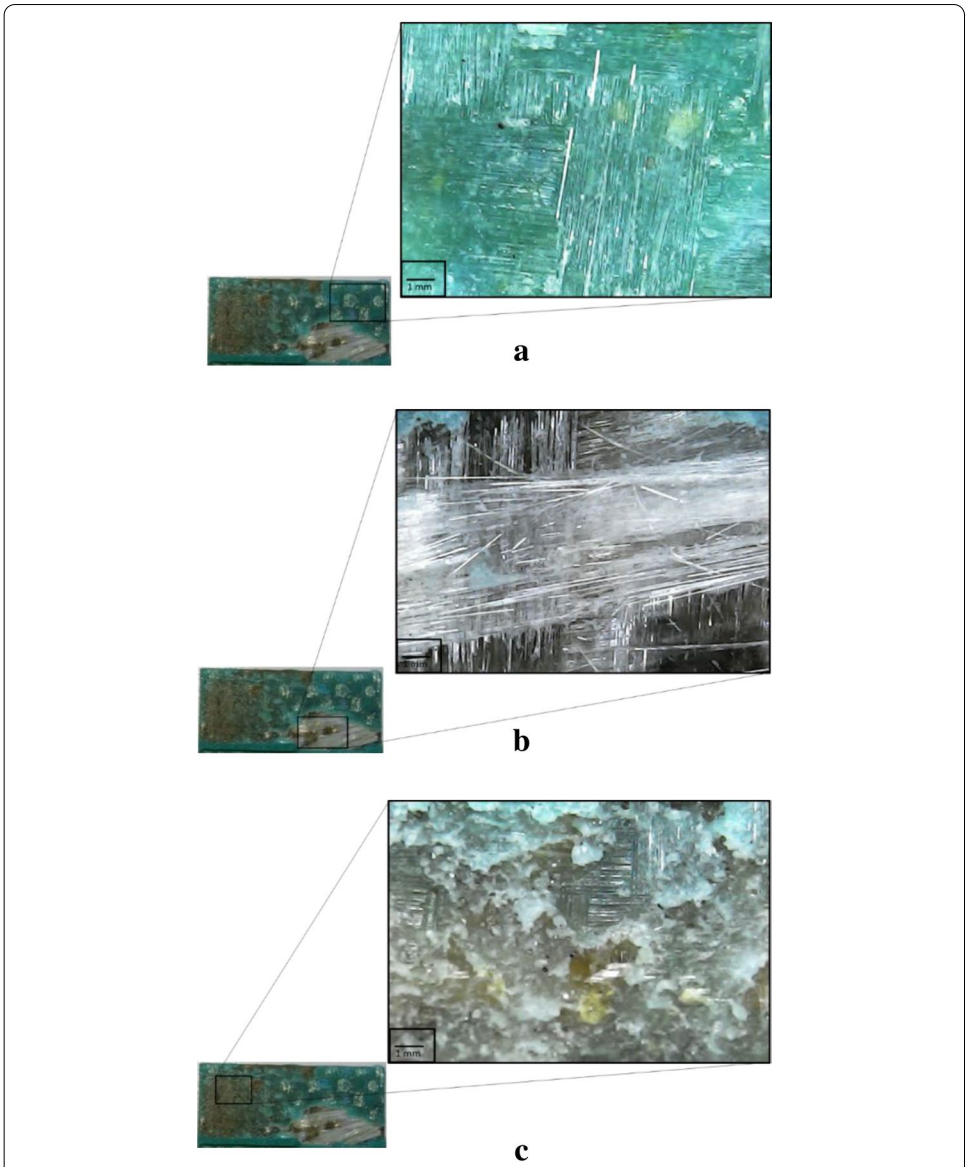

Fig. 6 Microscope images of areas of the hybrid 2-layer bonded joint failure surface, **a** generalized LFT, **b** generalized delamination and **c** TLC/LFT mixed mode

Figure 8 presents a schematic of the general crack path as a function of synthetic envelope. It can be seen from Fig. 8a that the general crack path for the hybrid 2-layer bonded joint followed an initial TLC/LFT mixed modes close to the interface of one of the adherends followed by a small cohesive transition zone through the adhesive layer towards the interface of the opposite adherend. There, the failure modes changed to a generalized LFT and delamination across the failure surface. This delamination penetrated both synthetic layers. For the hybrid 3-layer bonded joint, Fig. 8b depicts the general crack path. The path began close to the interface of one of the adherends with a COH/LFT mixed mode, progressing to a relatively large cohesive transition zone

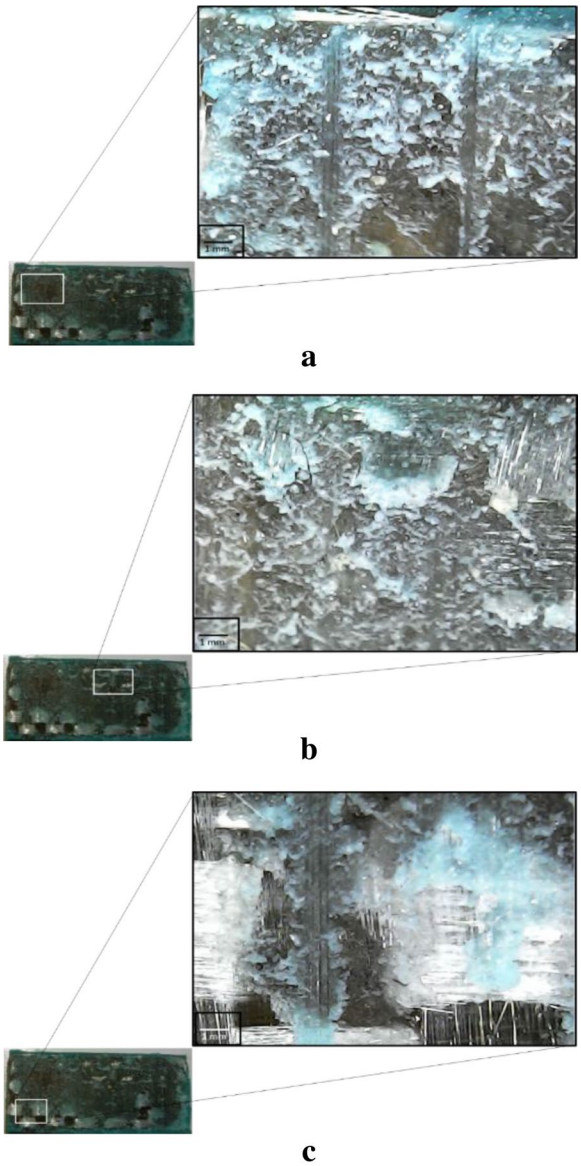

Fig. 7 Magnified view of areas of the hybrid 3-layer bonded joint failure surface, **a** COH, **b** COH/LFT mixed mode and **c** TLC/LFT mixed mode

towards the adhesive/adherend interface of the opposite adherend. Finally, it ended with a TLC/LFT mixed mode close to the interface.

Effect of adherend type on the bonded joint performance

Figure 9 presents representative load–displacement curves of SLJs as a function of adherend material, while Table 3 summarizes the data obtained from the test. It can be seen that the performance of the joints significantly varied. This is explained by the difference in the adhered material properties (see Table 2). The pure jute joint (JFRP), presented the lowest failure load as expected, as the pure jute adherends had the lowest properties and the SLJs failed in the adherends (see Fig. 4d and e). The hybrid

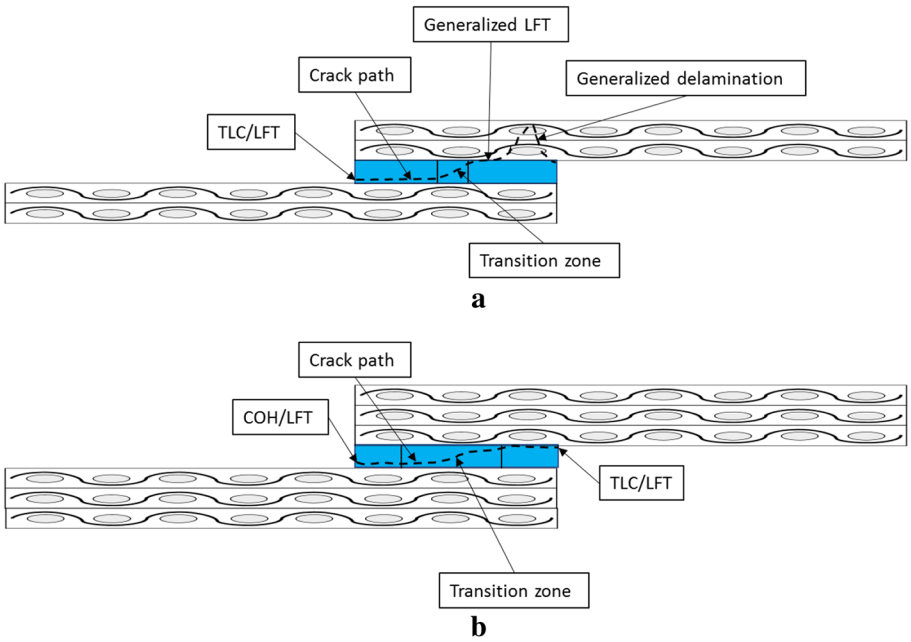

Fig. 8 Scheme of the general crack path and failure mode of the hybrid natural/synthetic bonded joints, **a** $G_2J_5G_2$ SLJs (hybrid 2-layer case); **b** $G_3J_5G_3$ SLJs (hybrid 3-layer case)

2-layer SLJs presented an improvement in average failure load when compared to the JFRP of approx. 27%, while the hybrid 3-layer SLJs presented an increase of failure load of approx. 48% when compared to JFRP. Furthermore, if the hybrid SLJs performance is compared, it was found that the failure load of the hybrid SLJs was significantly affected by the number of synthetic layers (i.e. an increase in average failure load of approx. 28% was found when the hybrid 3-layer SLJ is compared to the 2-layer joint). This is explained by the difference in the adherend material properties and its effect on the joint failure modes as increased material properties, (i.e. composite stiffness and transverse tensile strength), help mitigate tip rotation during shear loading as well as delamination failure onset. As described in the previous section, the failure mode of the hybrid 3-layer joint was defined by symmetrical LFT fronts from the overlap edges that progressed to LFT/COH mixed modes in the middle of the overlap. This is similar to the failure mode observed for the pure synthetic (GFRP) SLJs. Similar mixed failure modes were observed in the literature for GFRP joints [35]. On the other hand, the hybrid 2-layer joint failure mode displayed significant localized delamination on the overlap edge. Local delamination is linked to catastrophic failure of the global structure [1]. Therefore, the improved adherend properties of the hybrid 3-layer composite likely avoided localized delamination failure due to increased transverse tensile strength as well as bending stiffness [36].

To summarize, the hybrid 3-layer ($G_3J_5G_3$) SLJs reached a compromise of adherend properties, which avoided the delamination failure-onset compared to the hybrid 2-layer joint counterpart. Therefore, the hybrid 3-layer joint managed to match the bonded joint performance of GFRP adherends.

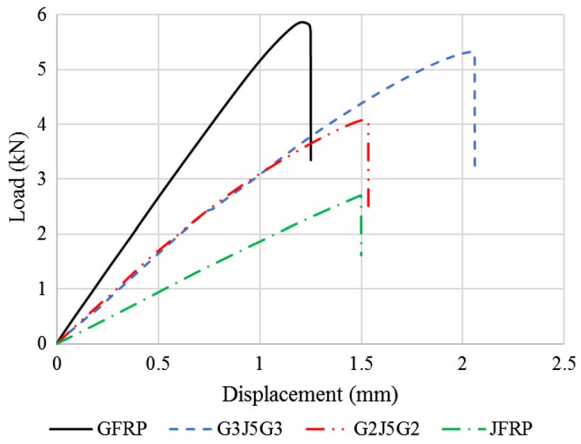

Fig. 9 Representative load–displacement curves of SLJs as a function of adherend material

Similar to the failure load, the rigidity of the joints also varied as a function of the adherend material, going from highest for the GFRP joints to lowest for the JFRP joints. The pure jute joint (JFRP), presented the lowest joint rigidity and a completely brittle behaviour. The lower ductility of the jute composite does not accommodate the overlap edge rotation due to load-axis eccentricity, therefore, it fails catastrophically earlier in the displacement.

The significant change in behaviour and joint rigidity observed for the GFRP, when compared to the hybrid joint cases, may be explained by the nearly twofold increase in adherend rigidity (from approx. 10 GPa to 20 GPa), as seen in Table 2. Such a high adherend rigidity translates in lower tip rotation, which in turn, generates lower peak peel stresses at the overlap edge and these are responsible for damage onset. This has been observed in the literature, where an increase in the bending stiffness of the adherend material postpones damage initiation and consequently increases joint failure load [4, 6]. However, the hybrid cases (i.e. hybrid 2- and 3-layer bonded joint cases) presented identical joint rigidity up to a certain displacement (~ 1.2 mm). This is due to an earlier damage onset in the hybrid 2-layer joint.

Figure 10 presents a comparison between adherend weight and joint failure load. It can be seen that the hybridization technique in the form of a 5-layer jute core sandwiched between 3 layers of glass had a significant impact on the average failure load to adherend weight ratio. This exemplifies the potential gains in weight savings and

Table 3 Data of the purely synthetic, hybrid and purely natural SLJs

Joint type	Average failure load (kN)	Average displacement (mm)	Adherend weight (g)	Average failure load/ Adherend weight ratio (kN/g)
GFRP-GFRP	5.51 ± 0.27	1.53 ± 0.29	14.41	0.38
$G_3J_5G_3$- $G_3J_5G_3$	5.53 ± 0.18	2.74 ± 0.83	12.06	0.46
$G_2J_5G_2$- $G_2J_5G_2$	3.95 ± 0.50	1.55 ± 0.33	11.98	0.33
JFRP-JFRP	2.89 ± 0.19	1.37 ± 0.19	9.86	0.29

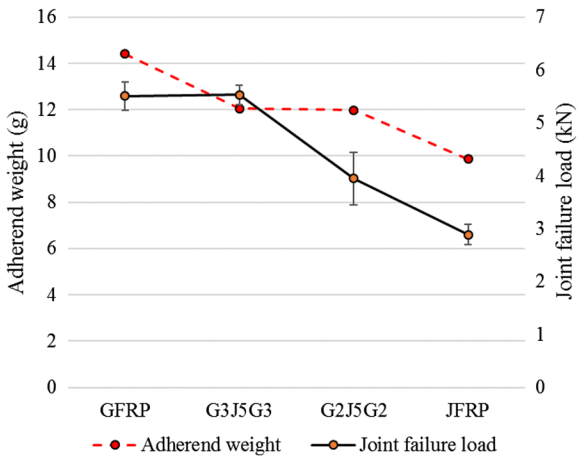

Fig. 10 Comparison between adherend weight and joint failure load

possible lowered fuel consumption with the application of this material in the automotive industry where high strength to weight ratio are important.

It should be noted that the interlaminar hybridization of jute composites with 2-layer glass fibre fabrics was appointed in the literature as an optimum compromise between material properties and weight/cost [37]. However, this research demonstrates that, this is no longer true when adhesively bonded joints are concerned. The addition of another glass layer is necessary to reach the adherend stiffness/peel stresses balance for the maximum joint performance to be achieved.

Conclusions

In this study single-lap adhesively bonded joints made of natural, synthetic and interlaminar hybrid fibre-reinforced polymer composites were experimentally investigated. The effect of the number of the interlaminar synthetic layers required to match the bonded joint efficiency of a fully synthetic GFRP bonded joint was studied by testing SLJs bonded with a modern tough structural adhesive used in the automotive The following conclusions can be drawn:

- A significant variation of joint behaviour was observed as a function of adherend material. The failure load of the hybrid adherend joints increased by increasing the number of external synthetic layers (i.e. the failure load of hybrid 3-layer joint increased by 28.6% compared to hybrid 2-layer joint) and reached the pure synthetic adherends joints efficiency. This is due to the optimum compromise between the adherend material property (i.e. stiffness and strength) and a diminished bondline peel stress state.
- The failure modes of the bonded joints presented significant differences as a function of adherend material. The pure jute SLJs failed in the adherend. The hybrid 2-layer joint presented a mixed TLC/LFT as well as major delamination failures, while the hybrid 3-layer joint presented stable cohesive crack growth as well as mixed TLC/LFT, similar to pure synthetic SLJs failure mode.

- The hybrid 3-layer adherend joints presented a diminished weight when compared to pure synthetic adherend, thus a reduction of mass and increase in sustainability can be achieved without losing the joint efficiency.

Abbreviations

FRC: Fibre-reinforced composite; NFRC: Natural fibre-reinforced composite; GFRP: Glass fibre-reinforced plastic; JFRP: Jute fibre-reinforced plastic; SLJ: Single lap joint; $G_2J_5G_2$: Hybrid 2-layer bonded joint; $G_3J_5G_3$: Hybrid 3-layer bonded joint; TLC: Thin layer cohesive failure; LFT: Light fibre cohesive failure; COH: Cohesive failure.

Acknowledgements

Authors would like to acknowledge the support of the Brazilian Research Agencies CNPq, FAPERJ and Dow Brazil for supplying the adhesive.

Authors' contributions

HFMQ designed and performed the experiments and wrote the paper. DKKC analyzed the data. MDB carried out the revision and made relevant changes in the manuscript. All authors read and approved the final manuscript.

Funding

No funding was received.

Availability of data and materials

The data that support the findings of this study are available from the corresponding author, (MDB), upon reasonable request.

Competing interests

The authors declare that they have no competing interests.

Received: 23 November 2020 Accepted: 14 December 2020
Published online: 04 January 2021

References

1. Banea M, da Silva LF. Adhesively bonded joints in composite materials: an overview. Proc IMechE. 2009;223(1):1–18.
2. Budhe S, Banea M, De Barros S, Da Silva L. An updated review of adhesively bonded joints in composite materials. Int J Adhes Adhes. 2017;72:30–42.
3. Budhe S, Banea MD, de Barros S. Bonded repair of composite structures in aerospace application: a review on environmental issues. Appl Adhes Sci. 2018;6(1):3.
4. Banea MD. Influence of adherend properties on the strength of adhesively bonded joints. MRS Bull. 2019;44(8):625–9.
5. Banea MD, Rosioara M, Carbas RJC, da Silva LFM. Multi-material adhesive joints for automotive industry. Compos B Eng. 2018;151:71–7.
6. Banea MD, da Silva LFM, Carbas R, Campilho RDSG. Effect of material on the mechanical behaviour of adhesive joints for the automotive industry. J Adhes Sci Technol. 2017;31(6):663–76.
7. Pickering KL, Efendy MGA, Le TM. A review of recent developments in natural fibre composites and their mechanical performance. Compos A Appl Sci Manuf. 2016;83:98–112.
8. Budhe S, de Barros S, Banea M. Theoretical assessment of the elastic modulus of natural fiber-based intra-ply hybrid composites. J Braz Soc Mech Sci Eng. 2019;41(6):263.
9. Rohit K, Dixit S. A review-future aspect of natural fiber reinforced composite. Polym Renew Res. 2016;7(2):43–59.
10. Pereira AL, Banea MD, Pereira AB. Effect of intralaminar hybridization on mode I fracture toughness of natural fiber-reinforced composites. J Braz Soc Mech Sci Eng. 2020. https://doi.org/10.1007/s40430-020-02525-w.
11. de Araujo Alves Lima R, Kawasaki Cavalcanti D, de Souza e Silva Neto J, da Meneses Costa H, Banea MD. Effect of surface treatments on interfacial properties of natural intralaminar hybrid composites. Polym Compos. 2020;41(1):314–25.
12. Pereira AL, Banea MD, Neto JS, Cavalcanti DK. Mechanical and thermal characterization of natural intralaminar hybrid composites based on sisal. Polymers. 2020;12(4):866.
13. Cavalcanti D, Banea M, Neto J, Lima R, da Silva L, Carbas R. Mechanical characterization of intralaminar natural fibre-reinforced hybrid composites. Compos B Eng. 2019;175:107149.
14. Jawaid M, Abdul Khalil HPS. Cellulosic/synthetic fibre reinforced polymer hybrid composites: a review. Carbohyd Polym. 2011;86(1):1–18.
15. Ku H, Wang H, Pattarachaiyakoop N, Trada M. A review on the tensile properties of natural fiber reinforced polymer composites. Compos B Eng. 2011;42(4):856–73.
16. Sinha AK, Narang HK, Bhattacharya S. Mechanical properties of hybrid polymer composites: a review. J Braz Soc Mech Sci Eng. 2020;42(8):431.
17. Roe P, Ansell MP. Jute-reinforced polyester composites. J Mater Sci. 1985;20(11):4015–20.
18. Neto JSS, Lima RAA, Cavalcanti DKK, Souza JPB, Aguiar RAA, Banea MD. Effect of chemical treatment on the thermal properties of hybrid natural fiber-reinforced composites. J Appl Polym Sci. 2019;136(10):47154.

19. Campilho RDSG, Moura DC, Gonçalves DJS, da Silva JFMG, Banea MD, da Silva LFM. Fracture toughness determination of adhesive and co-cured joints in natural fibre composites. Compos B Eng. 2013;50:120–6.
20. de Queiroz HFM, Banea MD, Cavalcanti DKK. Experimental analysis of adhesively bonded joints in synthetic- and natural fibre-reinforced polymer composites. J Compos Mater. 2020;54(9):1245–55.
21. Gonzalez-Murillo C, Ansell MP. Co-cured in-line joints for natural fibre composites. Compos Sci Technol. 2010;70(3):442–9.
22. Melese KG, Singh I. Joining behavior of jute/sisal fibers based epoxy laminates using different joint configurations. J Nat Fibers. 2020. https://doi.org/10.1080/15440478.2020.1798843.
23. Mittal A, Deb A, Chou C. A study into the mechanical behavior of adhesively-bonded jute fiber-reinforced composite. SAE Int J Mater Manf. 2015. https://doi.org/10.4271/2015-01-0729.
24. Mostafa NH. Tensile and fatigue properties of Jute-Glass hybrid fibre reinforced epoxy composites. Mater Res Express. 2019;6(8):085102.
25. Ramesh M, Palanikumar K, Reddy KH. Mechanical property evaluation of sisal–jute–glass fiber reinforced polyester composites. Compos B Eng. 2013;48:1–9.
26. Yoon HC, Wang RL, Jeon YB, Choi JY, Lee SY, Thai PQ, et al. Effects of adhesive joint on the failure strength properties of natural fiber reinforced composite. Key Eng Mater. 2007;353–358:1960–4.
27. Ferreira JM, Silva H, Costa JD, Richardson A. Stress analysis of lap joints involving natural fibre reinforced interface layers. Compos Part B-Eng. 2005;36(1):1–7.
28. dos Reis M, Banea M, da Silva L, Carbas R. Mechanical characterization of a modern epoxy adhesive for automotive industry. J Braz Soc Mech Sci Eng. 2019;41(8):340.
29. Bonaldo J, Banea M, Carbas R, Da Silva L, De Barros S. Functionally graded adhesive joints by using thermally expandable particles. J Adhes. 2019;95(11):995–1014.
30. Neto JSS, Banea MD, Cavalcanti DKK, Queiroz HFM, Aguiar RAA. Analysis of mechanical and thermal properties of epoxy multiwalled carbon nanocomposites. J Compos Mater. 2020;54(30):4831–40.
31. Banea MD, da Silva LF, Campilho RD. Moulds design for adhesive bulk and joint specimens manufacturing. Assem Autom. 2012;32(3):284–92.
32. Budhe S, Ghumatkar A, Birajdar N, Banea MD. Effect of surface roughness using different adherend materials on the adhesive bond strength. Appl Adhes Sci. 2015;3(1):20.
33. ASTM International. Standard practice for classifying failure modes in fiber-reinforced-plastic (FRP) joints. West Conshohocken: ASTM International; 2019. https://doi.org/10.1520/D5573-99R19
34. Sousa JM, Correia JR, Gonilha J, Cabral-Fonseca S, Firmo JP, Keller T. Durability of adhesively bonded joints between pultruded GFRP adherends under hygrothermal and natural ageing. Compos B Eng. 2019;158:475–88.
35. Hunter-Alarcón RA, Vizán A, Peréz J, Leyrer J, Hidalgo P, Pavez B, et al. Effect of the natural aging process on the shear strength of FRP composite single lap joints. Int J Adhes Adhes. 2018;86:4–12.
36. Blackman BRK, Kinloch AJ, Rodriguez-Sanchez FS, Teo WS. The fracture behaviour of adhesively-bonded composite joints: Effects of rate of test and mode of loading. Int J Solids Struct. 2012;49(13):1434–52.
37. Ahmed KS, Vijayarangan S. Tensile, flexural and interlaminar shear properties of woven jute and jute-glass fabric reinforced polyester composites. J Mater Process Technol. 2008;207(1):330–5.

Publisher's Note